Helium at nonzero temperatures: A variational density-matrix approach for Bose fluids

G. Senger
Institut für Theoretische Physik, Universität zu Köln, D-5000 Köln 41, West Germany

M. L. Ristig*
School of Physics, The University of New South Wales Kensington, New South Wales, Australia 2033

K. E. Kürten*
Courant Institute of Mathematical Sciences, New York University, 251 Mercer Street, New York, New York 10012

C. E. Campbell
School of Physics and Astronomy, University of Minnesota, 116 Church Street S.E., Minneapolis, Minnesota 55455
(Received 12 August 1985)

A variational statistical mechanics of boson quantum fluids such as ^{4}He is developed as a natural generalization of the Jastrow Euler-Lagrange method which has been successfully applied to the ground-state problem. The results include a quantitative description of the liquid-gas portion of the phase diagram, including the corresponding critical point and spinodal line. Also calculated is the temperature dependence of the liquid structure function and phonon-roton spectrum within the class of trial density matrices explored in this work.

I. INTRODUCTION

Recent substantial advances in the microscopic description of dense quantum fluids at zero temperature[1] are vigorously calling for suitable generalizations of the now available *ab initio* approaches to deal with excited states of quantum systems and their thermal properties.[2–6] Such a quantitative microscopic theory of quantum fluids at finite temperatures may be developed by an appropriate generalization of the Feenberg-Jastrow variational approach.[7,8] This formalism has led to a thorough explanation of the ground-state structure of strongly correlated many-body systems described by a Hamiltonian of the form

$$H=T+V=-\sum_{i=1}^{N}\frac{\hbar^2}{2m}\nabla_i^2+\sum_{\substack{i,j=1\\ i<j}}^{N}v(r_{ij})\ , \tag{1}$$

where the potential $v(r)$ represents the bare interparticle interaction. For bosons this theory rests on the choice of an appropriate set of trial wave functions for the many-body ground state, which in the simplest case take the Jastrow form

$$\Psi(\underline{R})=\frac{1}{\sqrt{\mathcal{N}}}\exp\left[\frac{1}{2}\sum_{\substack{i,j=1\\ i<j}}^{N}u(r_{ij})\right]\ , \tag{2}$$

where $\underline{R}=(\mathbf{r}_1,\mathbf{r}_2,\ldots,\mathbf{r}_N)$. The unit-normalized wave function (2) represents a first plausible ansatz but may be systematically improved by adopting more complex Feenberg functions which include triple-correlation terms $u_3(\mathbf{r}_i,\mathbf{r}_j,\mathbf{r}_k)$, etc., in the exponential.[9–11]

To work within a dynamically consistent approach[7] the ground-state wave function (2) or the more sophisticated Feenberg function is then determined by invoking the minimum principle for the ground-state energy,[12,10]

$$E_0\le E=\langle\Psi\,|\,H\,|\,\Psi\rangle\ . \tag{3}$$

The statistical mechanics of quantum fluids at nonzero temperatures may be worked out in an analogous manner. Instead of employing a set of trial wave functions (2), one begins with an appropriate set of trial density matrices which may take account of incoherence effects in the finite-temperature systems. Next, one proceeds by optimizing the Helmholtz free energy employing the Gibbs-Delbrück-Moliere minimum principle.[13]

The first few steps along these lines have been described in Refs. 14–17. Here, we shall report on our present formal realization of this program by introducing the variational principle as the method for determining the choice of density matrix in a specified function space. We describe calculations of the various phase diagrams, structure function, and excitation energies for liquid helium within this formal frame. It should be considered as a first stage in this development since the minimal application is based at the moment on a rather crude approximation for the entropy; this approximation holds at sufficiently low temperatures when the number of elementary excitations is small compared with the total number of bosons so that the excitations are well represented as temperature-dependent elementary excitations at the level of Bijl-Feynman excitations. We stress, however, that the variational formalism put forward is not limited to this restricted region in phase space since we may systematically remove the restrictions set by the approximation.[18]

In Sec. II we describe the ansatz for the density matrix and develop its consequences by evaluating the associated internal energy, entropy, and Helmholtz free energy. The

latter functional is optimized in Sec. III to determine the best trial density matrix within the function space tested. The procedure leads to a coupled set of Euler-Lagrange equations which generate the structure function and excitation energies of the boson system at given density and temperature. Sections IV and V collect our main numerical results on these functions and on the phase diagram for liquid ^{4}He. In Sec. VI we present a heuristic phenomenological extension of the present model which permits a qualitative discussion of the phase equilibrium between liquid and vapor. Section VII contains a discussion of our principal results and approximations, and methods for improving the approximations and extending this approach.

II. DENSITY MATRIX AND THE HELMHOLTZ FREE ENERGY

Our formal analysis of the equilibrium properties of a boson fluid at nonzero temperatures is based on the Gibbs-Delbrück-Molière minimum principle for the trial Helmholtz free energy F. It is bound from below by the true free energy F_0 of the system,

$$F_0 \leq F = \mathrm{Tr}(HW) + \beta^{-1}\,\mathrm{Tr}(W \ln W) \tag{4}$$

with the inverse temperature $\beta = 1/k_B T$ and an equilibrium density operator W on the Hilbert space of the Hamiltonian (1) with appropriate statistics.[13] The operator W must be non-negative, satisfy boson statistics, and be normalized to unity: $\mathrm{Tr}\,W = 1$.

To most conveniently take account of the strong spatial correlations between the particles induced by the strong, short-range interaction, we employ the coordinate space representation and cast the matrix elements of the statistical operator W into the completely general form

$$W(\underline{R},\underline{R}') = \Phi(\underline{R})Q(\underline{R},\underline{R}')\Phi(\underline{R}') \,. \tag{5}$$

The incoherence factor Q contains no factors which depend only on primed or unprimed coordinates alone and it reduces to unity at vanishing temperature. In this case the function $\Phi(\underline{R})$ represents the ground-state wave function of the system.

For bosons the simplest class of trial functions Φ is of the Jastrow form (2). On the same level of sophistication the incoherence factor $Q(\underline{R},\underline{R}')$ is chosen to be represented by

$$Q(\underline{R},\underline{R}') = \exp\left[\sum_{i,j=1}^{N} \gamma(|\mathbf{r}_i - \mathbf{r}'_j|)\right] . \tag{6}$$

Employing the density fluctuation operators $\rho_{\mathbf{k}} = \sum_{i=1}^{N} \exp(i\mathbf{k}\cdot\mathbf{r}_i)$ we may write, equivalently,

$$Q(\underline{R},\underline{R}') = \exp\left[\frac{1}{N}\sum_{\mathbf{k}}{}' \gamma(k)\rho_{\mathbf{k}}(\underline{R})\rho_{-\mathbf{k}}(\underline{R}')\right] , \tag{7}$$

where terms with $k=0$ are omitted in the sum. Expression (7) shows that the trial density operator W thus constructed is non-negative if we require the Fourier inverse $\gamma(k)$ of the function $\gamma(r)$ to be non-negative. This is easily seen since all matrix elements of the operator W with respect to arbitrary states in the Hilbert space are non-negative in this case.[14] We observe further that the coordinate-space matrix elements $W(\underline{R},\underline{R}')$ are all positive or zero.[14] The Jastrow ansatz for functions $\Phi(\underline{R})$ and $Q(\underline{R},\underline{R}')$ has been explored earlier by Reatto and Chester,[19] by Feenberg[20] and in some more recent studies by DeMichelis, Masserini, and Reatto.[21,22] The particular ansatz chosen for the statistical operator should permit an adequate description of the superfluid phases of a many-boson system. However, since it leads necessarily to a nonvanishing condensate fraction, the Jastrow ansatz is not sufficiently flexible to also provide an appropriate representation of the normal phases.

To proceed further it is slightly more convenient to write the trial density matrix in coordinate space as

$$W(\underline{R},\underline{R}') = \psi(\underline{R})P(\underline{R},\underline{R}')\psi(\underline{R}') \,, \tag{8}$$

where the unit-normalized function $\Psi(\underline{R})$ is represented by expression (2). Then,

$$P(\underline{R},\underline{R}') = \exp\left[\sum_{i,j=1}^{N} \gamma(|\mathbf{r}_i - \mathbf{r}'_j|) - \tfrac{1}{2}\sum_{i,j=1}^{N} \gamma(r_{ij}) - \tfrac{1}{2}\sum_{i,j=1}^{N} \gamma(r'_{ij})\right] \tag{9}$$

has unit-normalized diagonal elements, $P(\underline{R},\underline{R}) = 1$, and, consequently, the diagonal part of the density operator is given by $W(\underline{R},\underline{R}) = \Psi^2(\underline{R})$ with $\mathrm{Tr}\,W = 1$.

Our next task will be to evaluate the internal energy $U = \mathrm{Tr}HW$ and the entropy $TS = -\beta^{-1}\mathrm{Tr}(W \ln W)$ and therewith the trial Helmholtz free energy (4) as explicit functionals of the quantities $\gamma(r)$ and $u(r)$ characterizing our trial density matrix. The internal energy may be evaluated by following the standard Jackson-Feenberg procedure[7] yielding an energy per particle

$$\frac{U}{N} = \frac{\rho}{2}\int v^*(r)g(r)d^3r + \frac{1}{(2\pi)^3\rho}\int \epsilon_0(k)\gamma(k)d^3k \,. \tag{10}$$

The effective potential $v^*(r)$ is defined by

$$v^*(r) = v(r) - \frac{\hbar^2}{4m}\nabla^2 u(r) \,, \tag{11}$$

$\epsilon_0(k) = \hbar^2 k^2/2m$ is the single-particle energy of independent bosons and the radial distribution function $g(r)$ is associated with the diagonal part, $W(\underline{R},\underline{R}) = \Psi^2(\underline{R})$, of the density matrix adopted here.

To evaluate the entropy we need the trace of $W \ln W$. Instead of taking the trace directly, we first evaluate the traces of powers of the density operator. These traces are represented by the integrals

$$\mathrm{Tr}W^{m+1}=\int d\underline{R}_1\int\cdots\int d\underline{R}_{m+1}\Psi^2(\underline{R}_1)\cdots\Psi^2(\underline{R}_{m+1})\left[\prod_{\substack{\mathbf{k}\\(k_x>0)}}\exp G^{(m)}\right]$$

$$\equiv\left\langle\prod_{\mathbf{k}}{}'\exp G^{(m)}\right\rangle , \tag{12}$$

where the functions $G^{(m)}$ are quadratic expressions in the density fluctuations ρ_k,

$$G^{(m)}(\mathbf{k},\underline{R}_\alpha)=-\frac{1}{N}\gamma(k)[\,|\rho_{\mathbf{k}}(\underline{R}_1)-\rho_{\mathbf{k}}(\underline{R}_2)|^2+\cdots$$

$$+|\rho_{\mathbf{k}}(\underline{R}_{m+1})-\rho_{\mathbf{k}}(\underline{R}_1)|^2] \tag{13}$$

and m may be any non-negative integer. The product has to be taken over the positive half-space ($k_x>0$) which is indicated by a prime on the product in the second line of Eq. (12). The expression (13) may be written in a more compact form upon introducing an $(m+1)\times(m+1)$ matrix $M^{(m)}$ having the elements $M_{\alpha,\beta}=2\delta_{\alpha,\beta}-\delta_{\alpha,\beta+1}-\delta_{\beta,\alpha+1}$ with the cyclic condition $m+2=1$,

$$G^{(m)}=-\frac{1}{N}\gamma(k)\sum_{\alpha,\beta=1}^{m+1}\rho_{\mathbf{k}}(\underline{R}_\alpha)M^{(m)}_{\alpha\beta}\rho_{-\mathbf{k}}(\underline{R}_\beta) . \tag{14}$$

The integrals (12) can be viewed as standard normalization integrals associated with a boson mixture of $m+1$ differing components which are correlated in a cyclic manner. Standard methods of statistical mechanics are available to study and to evaluate (at least in principle) such integrals.[23,24] The results are of the general form,

$$\mathrm{Tr}W^{m+1}=\exp[ND(m)] , \tag{15}$$

where quantity D is of order N^0 in the thermodynamic limit and is a discrete function of the integer m. It is plausible to assume that this function, known at discrete points m, may be continued analytically along the entire positive real axis α. If that is the case then the function $D(\alpha)$, α real and positive, may be used to derive the desired expression for the entropy by invoking the identity

$$\frac{\partial}{\partial\alpha}\mathrm{Tr}W^{\alpha+1}\bigg|_{\alpha=0}=\mathrm{Tr}(W\ln W) . \tag{16}$$

Consequently, the entropy per particle then follows as

$$\frac{TS}{N}=-\frac{1}{\beta N}\frac{\partial}{\partial\alpha}[\exp ND(\alpha)]\bigg|_{\alpha=0}=-\frac{1}{\beta}\dot{D} , \tag{17}$$

where $\dot{D}=\partial D(\alpha)/\partial\alpha\,|_{\alpha=0}$ and $D(0)=0$.

Thus, the central task to perform is the evaluation of function $D(m)$ and to achieve its analytic continuation. At present we do this by adopting a simple approximation which disregards the effects of correlations between entropy fluctuations. The approximation is based on the separability assumption which is known to be accurate only at low temperatures.[20] It has been used with success in the iterative step of the paired phonon analysis of the ground state of a boson system.[11,12] The assumption reads[14]

$$\left\langle\prod_{\mathbf{k}}{}'\exp G^{(m)}\right\rangle\simeq\prod_{\mathbf{k}}{}'\langle\exp G^{(m)}\rangle \tag{18}$$

which leads, via Eqs. (12) and (15), to the approximate expression

$$D(m)\simeq D_0(m)=\frac{1}{N}\sum_{\mathbf{k}}{}'\ln\langle\exp G^{(m)}\rangle . \tag{19}$$

The average value on the right-hand side of Eq. (19) has been calculated in Ref. 25 and yields

$$D_0(m)=-\frac{1}{N}\sum_{\mathbf{k}}{}'\ln\det[1+\gamma(k)S(k)M^{(m)}] , \tag{20}$$

where $S(k)$ is the static liquid structure function associated with the radial distribution function $g(r)$ introduced above.

The determinant of the $(m+1)\times(m+1)$ matrix $1+\gamma(k)S(k)M^{(m)}$ may be evaluated by taking the product of the corresponding $m+1$ eigenvalues.[17] The eigenvalues of the matrix $M^{(m)}$ are

$$M_l^{(m)}=4\sin^2[l\pi/(m+1)] \tag{21}$$

($l=1,2,\ldots,m+1$). Introducing a non-negative function $n(k)$ in Fourier space,

$$n(k)[1+n(k)]=\gamma(k)S(k) , \tag{22}$$

we may cast Eq. (20) into

$$D_0(m)=-\frac{1}{N}\sum_{\mathbf{k}}{}'\ln\left\{\prod_{l=1}^{m}\left[1+4n(k)[1+n(k)]\sin^2\left[\frac{l\pi}{m+1}\right]\right]\right\} . \tag{23}$$

The product appearing in the logarithm in Eq. (23) may be shown to represent a $2m$-fold polynomial of the form $[(1+n)^{1+m}-n^{1+m}]^2$. Thus, inserting this expression into result (23) we may analytically continue and arrive at the function

$$D_0(\alpha)=-\frac{1}{N}\sum_{\mathbf{k}}\ln\{[1+n(k)]^{1+\alpha}-[n(k)]^{1+\alpha}\} . \tag{24}$$

According to prescription (17) the entropy per particle in the separability approximation follows as

$$\frac{TS}{N}\simeq\frac{TS_0}{N}=\frac{1}{\beta N}\sum_{\mathbf{k}}\{[1+n(k)]\ln[1+n(k)]$$

$$-n(k)\ln n(k)\} . \tag{25}$$

The trial Helmholtz free energy may therefore be decomposed into the parts

$$\frac{F}{N}=\frac{U}{N}-\frac{TS_0}{N}+\frac{1}{\beta}\dot{D}_1 , \tag{26}$$

where the internal energy and the first entropy portion are explicitly given by Eqs. (10) and (25). The dotted quantity $\dot{D}_1$ vanishes at sufficiently low temperatures but must be included if we approach the lambda transition line from the low-temperature side in order to give a realistic microscopic description in this region of phase space. We hope to present an explicit evaluation of this contribution to the free energy in the near future.

To conclude this section we write the internal energy (10) in terms of the derived quantities $g(r)$ and $n(k)$ by employing the relation (22),

$$\frac{U}{N}=\frac{\rho}{2}\int v^*(r)g(r)d^3r-\frac{1}{2(2\pi)^3\rho}\int \tilde{\omega}^*(k)S(k)d^3k , \tag{27}$$

where we have introduced a quantity

$$\tilde{\omega}^*(k)=\tfrac{1}{2}\epsilon_0(k)S^{-2}(k)\{1-[1+2n(k)]^2\} \tag{28}$$

which vanishes as $T\rightarrow 0$.

III. OPTIMIZATION

For the next major step we minimize the trial Helmholtz free energy (26) by choosing the optimal real functions $\gamma(r)$ and $u(r)$ which determine the adopted form of the trial density matrix. These optimal functions are solutions of two coupled Euler-Lagrange equations

$$\frac{\delta F}{\delta\gamma(r)}=0, \quad \frac{\delta F}{\delta u(r)}=0 . \tag{29}$$

At present we ignore the contribution $\dot{D}_1$ in Eq. (26) varying only the explicitly available expressions (25) and (27). Straightforward variation of the energy F with respect to the incoherence term $\gamma(r)$ leads us to the relation

$$\beta\epsilon_0(1+2n)S^{-1}=\ln(1+n)-\ln n , \tag{30}$$

where the quantities depend on the wave number k. Equation (30) may be converted into the more useful form

$$\epsilon_0(k)=S(k)\epsilon(k)\tanh[\tfrac{1}{2}\beta\epsilon(k)] \tag{31}$$

by introducing the energies $\epsilon(k)$ via the relation

$$n(k)=\frac{1}{\exp[\beta\epsilon(k)]-1} . \tag{32}$$

In the limit $T\rightarrow 0$ we recover from result (31) the familiar Bijl-Feynman relation between the static structure function and the elementary excitation energies in the absence of backflow. This suggests that we may interpret the solution $\epsilon(k)$ as the simplest temperature-dependent generalization of the Bijl-Feynman excitation spectrum. We should note in this context that, since $S(k)$ and $\gamma(k)>0$, these energies are non-negative as are the occupation probabilities. The particularly simple result (30) or (31) is of course a direct consequence of our separability approximation for the entropy. The significance of result (31) is most clearly reflected in the observation that the dynamic structure function χ'' consistent with Eq. (31) is generated by a single resonance positive frequency mode at given density and temperature,[26]

$$S(k,\omega)=\frac{2}{1-\exp(-\beta\omega)}\chi''(k,\omega) , \tag{33}$$

where the response function χ'' is of the form

$$\chi''(k,\omega)=\epsilon_0(k)\frac{|\omega|}{\omega}\delta(\omega^2-\epsilon^2(k)) \tag{34}$$

involving the spectrum $\epsilon(k)$. We note that functions $S(k,\omega)$ and $\chi''(k,\omega)$ obey the familiar ω^n sum rules, $n=0$ and 1. Expression (33) demonstrates that the present approximation for the entropy suppresses backflow and multiexcitation interaction effects at any finite temperature, although it does incorporate temperature-dependent correlation effects due to the presence of thermally excited states.

Within the separability approximation the Helmholtz free energy may be varied with respect to the function $u(r)$ by following closely the paired phonon procedure familiar from studies of the ground state.[11,12] The variational result may be most efficiently expressed by employing a generalized structure function[7]

$$S(k;\alpha)=\frac{1}{N}\int d\underline{R}\,\rho_{\underline{k}}\rho_{-\underline{k}}W(\underline{R},\underline{R};\alpha) \tag{35}$$

and the radial distribution function $g(r;\alpha)$ associated with Eq. (35). The diagonal part $W(\underline{R},\underline{R};\alpha)$ of the generalized density operator $W(\alpha)$ appearing in Eq. (35) is defined by the square of the following unit-normalized wave function,

$$\Psi(\underline{R};\alpha)=\frac{1}{\sqrt{\mathcal{N}(\alpha)}}\times\prod_{\substack{i,j=1\\ i<j}}^{N}\exp(\tfrac{1}{2}\{u(r_{ij})+\alpha[v^*(r_{ij})+\omega^*(r_{ij})]\}) \tag{36}$$

being driven by the effective interactions (11) and (28). With the help of quantity (35) the Euler-Lagrange equation resulting from varying the free energy with respect to $u(r)$ now takes the form familiar from the paired phonon treatment at vanishing temperature,

$$\epsilon_0(k)[1-S(k)]=2\dot{S}(k) , \tag{37}$$

or, equivalently,

$$\frac{\hbar^2}{4m}\nabla^2 g(r)=\dot{g}(r) . \tag{38}$$

Functions $\dot{S}(k)$ and $\dot{g}(r)$ represent the derivatives of $S(k,\alpha)$ and $g(r,\alpha)$, respectively, with respect to the parameter α taken at $\alpha=0$.

To study the stability properties[27] as well as to design a practical iteration scheme for solving the Euler-Lagrange Eqs. (31) and (37), we combine Eqs. (31) and (28) by taking the square

$$\epsilon^2(k)=\epsilon_0^2(k)S^{-2}(k)[1+2n(k)]^2$$
$$=\epsilon_0(k)[S^{-2}(k)\epsilon_0(k)-2\tilde{\omega}^*(k)] \quad (39)$$

and then inserting condition (37), i.e., $\epsilon_0=2\dot{S}/(1-S)$, into Eq. (39). This manipulation generates the relation[28]

$$\epsilon(k)=\{\epsilon_0(k)[\epsilon_0(k)+2\tilde{\omega}(k)]\}^{1/2}, \quad (40)$$

where we have introduced a potential

$$2\tilde{\omega}(k)=[\epsilon_0(k)S(k)+2\dot{S}(k)]S^{-2}(k)-\epsilon_0(k)-2\tilde{\omega}^*(k) . \quad (41)$$

Equation (40) is of the standard Bogoliubov form[29] with function $\tilde{\omega}(k)$ being identified with the effective particle-hole potential[30] as $T\rightarrow 0$. Evidently, the boson system cannot be stable unless

$$\epsilon_0(k)+2\tilde{\omega}(k)>0 . \quad (42)$$

In particular, condition (42) reduces to

$$\tilde{\omega}(0)=mc^2>0 \quad (43)$$

at small values of wave number k where c is the isothermal velocity of ordinary second defined by the limit $\epsilon(k)=\hbar kc$ as $k\rightarrow 0$. If Eq. (43) is violated the system becomes unstable against long-wavelength density oscillations.

Equation (40) together with Eq. (31) is well suited for calculating the optimal excitation energies $\epsilon(k)$ and the optimal structure function $S(k)$ by iteration. What is needed to realize such an iteration scheme is an explicit relation between the generalized structure function $S(k;\alpha)$ or the radial distribution function $g(r;\alpha)$, the corresponding bare correlation functions ($\alpha=0$), and the variational functions $u(r)$ and $\gamma(r)$. At $T=0$ this relation is usually established within the hypernetted-chain analysis where the contributions of elementary diagrams are usually disregarded. We adopt the same approximation procedure at nonzero temperatures following the established lines familiar from the ground-state treatment. Employing the hypernetted-chain equations available for $S(k)$ and $\dot{S}(k)$ (Refs. 11 and 12) we may express the potential $v(r)$ or its dimensionless Fourier inverse $\tilde{v}(k)$ appearing in the central equation (40) and defined by Eq. (41) in terms of the radial distribution function $g(r)$ [or the structure function $S(k)$] and the effective interaction v^*, Eq. (28). A few algebraic manipulations lead to the expression[30]

$$v(r)=vg+\frac{\hbar^2}{m}(\nabla\sqrt{g})^2+(g-1)(w+v^*) \quad (44)$$

which involves an induced potential $w(r)$ described by the Fourier inverse

$$w(k)=-\tfrac{1}{2}\epsilon_0(k)[2S(k)+1][S(k)-1]^2S^{-2}(k) . \quad (45)$$

This induced potential is of the same form as the one which appears in the Lantto-Siemens equations for the optimal Jastrow ground-state trial function.[31] Indeed, inserting Eq. (44) into Eq. (40) and employing Eq. (31) we find, after more elementary algebraic manipulation, a Schrödinger-like equation for $\sqrt{g(r)}$, which acts as a two-body amplitude within the medium:

$$-\frac{\hbar^2}{m}\nabla^2\sqrt{g}+(v+w+v^*)\sqrt{g}=0 . \quad (46)$$

This constitutes the temperature-dependent generalization of the Lantto-Siemens equations of Ref. 31.

Once the optimal functions $S(k)$, $g(r)$, $n(k)$, $\epsilon(k)$, etc., are known as the calculation of the thermodynamic quantities such as internal energy [Eq. (27)], entropy [Eq. (25)], and Helmholtz free energy [Eq. (26)] is straightforward. We stress that for the optimal choice, Eq. (25) yields an entropy which exactly agrees with the result derived from taking the thermal derivative, i.e., $(\partial F/\partial T)_{V,N}$, of the free energy since quantity F is stationary. For the same reason the optimal chemical potential may be expressed as an integral containing only the functions $S(K)$ and $n(k)$ but not their derivatives with respect to density,

$$\mu=\rho\int v^*(r)g(r)d^3r+\frac{\rho}{2}\int v^*(r)[g(r)-1]d^3r$$
$$-\frac{1}{4(2\pi)^3\rho}\int\epsilon_0(k)S^{-2}(k)[S(k)-1]^3d^3k . \quad (47)$$

The same may be said for the pressure which follows from the thermodynamic relation $P=\rho\mu-F/V$.

IV. OPTIMAL STRUCTURE FUNCTION AND EXCITATION ENERGIES

A phenomenological study of the generalized Bijl-Feynman relation (31) has been given in Ref. 14. Here, we report on a detailed numerical study of the set of Euler-Lagrange equations (31) and (40) and of the variation of their solutions with temperature and density for bulk helium matter. The interparticle interaction is described by a Lennard-Jones potential with the standard set of parameters. To explore the thermodynamic behavior as a function of the helium mass we study the phase diagrams for ^{4}He, ^{6}He, and for helium atoms with the hypothetical mass $\frac{2}{3}$ that of ^{4}He.

Since at the present stage we omit the effects of correlations between the entropy fluctuations (due to the separability assumption) and backflow effects in the ground state as well as at elevated temperatures, a comparison with experimental data on liquid and gaseous helium can be at best semiquantitative. But despite the limited applicability of the present microscopic model to a description of real helium it is important to study its behavior in the entire phase space, at any temperature and density in order to be able to improve upon the present approximations at a later stage.

The Euler-Lagrange equations are solved numerically by iterating Eq. (40) in conjunction with relations (31) and (41). At each iterative step the input functions $S(k)$ and $\dot{S}(k)$ are calculated in the hypernetted-chain approximation by solving the standard hypernetted-chain equations which correspond to both quantities.[27] The T-ρ diagram, Fig. 1, shows that for the three differing masses considered, stable solutions exist only outside of certain regions of the phase diagram. The curves separating the re-

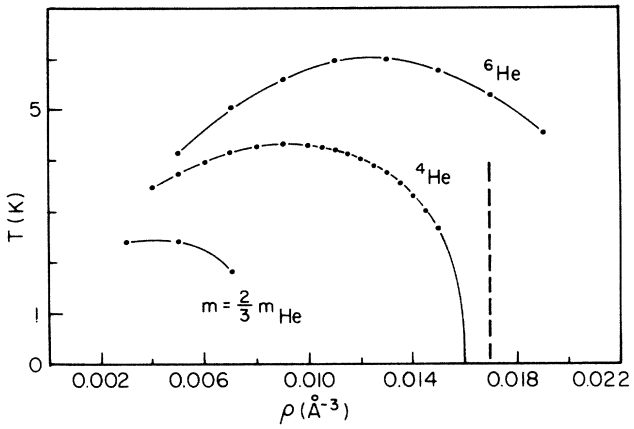

FIG. 1. Calculated isothermal spinodal line for ^{4}He fluid, ^{6}He fluid, and the fictitious boson isotope of helium with mass $\frac{2}{3}$ that of ^{4}He. The nearly vertical dashed line is the phase equilibrium line between liquid ^{4}He and the vacuum as described by the optimum trial density matrix studied in this work.

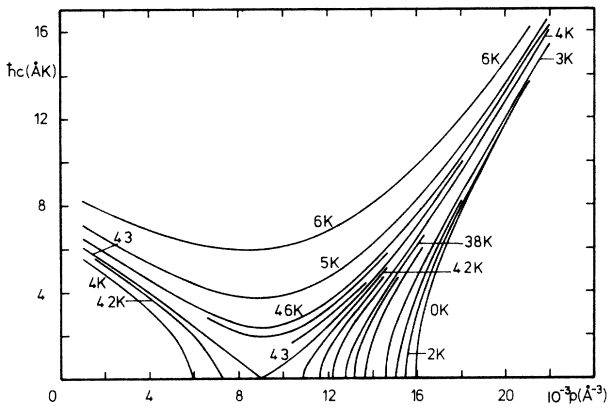

FIG. 2. Calculated isotherms of the isothermal sound velocity for ^{4}He fluid.

gions where physically admissible solutions are found from those where the condition (42) is violated represent the spinodal lines of the three different systems. On these lines the (isothermal) velocity of sound approaches zero thus indicating that the systems become unstable against density fluctuations at large wavelength. The spinodal point for ^{4}He at zero temperature appears at a density 0.016 Å^{-3} which is in agreement with earlier findings.[32] The maximum points of the various spinodal lines are identified as the model critical points for the first-order liquid-gas phase transition. For ^{4}He we find the critical data, $T_c \simeq 4.3$ K and $\rho_c \simeq 0.009$ Å^{-3}, which are fairly close to the experimental data for ^{4}He of $T_c \simeq 5.2$ K and $\rho_c \simeq 0.010$ Å^{-3}.[33] Since the kinetic energy becomes more important than the interaction energy if the particle mass decreases we expect and, indeed, find numerically that the instability region for mass $\frac{2}{3}$ the mass of ^{4}He is significantly smaller than for ^{4}He and ^{6}He and disappears eventually for still lighter masses slightly smaller than $0.1 m_4$, consistent with the conclusions of the quantum theory of corresponding states prediction for the disappearance of the critical point.[33]

On the liquid side of the spinodal curves, i.e., at densities exceeding the critical density, we find that the phonon velocity increases rapidly with density, thus becoming relatively independent of temperature at sufficiently high densities. This behavior is shown for ^{4}He matter in Fig. 2. On the gas side the velocity of the long-wavelength excitations increases with decreasing density and approaches the ideal gas data for sufficiently small densities. Figure 3 depicts the optimal excitation energies $\epsilon(k)$ for ^{4}He at temperature $T=6$ K and at various densities. At experimental equilibrium density ($\rho = 0.021\,85$ Å^{-3}) we obtain the typical phonon-roton form of the Bijl-Feynman spectrum with roton energies lying 2 to 3 times higher than experimentally observed, reflecting the fact that backflow effects are neglected in the present microscopic model. With decreasing density the roton minimum shifts to lower wave numbers, gradually weakening and disappearing at a density of about $\rho = 0.016$ Å^{-3}. At still lower densities the excitation curves increase monotonically with momentum $\hbar k$ and approach the free particle spectrum $\hbar^2 k^2/2m$ at wave numbers $k \geq 2$ Å^{-1} (crosses in Fig. 3). However, the linear phonon behavior of the excitations is correctly recovered at sufficiently small k values at all densities considered. The dependence of the excitation en-

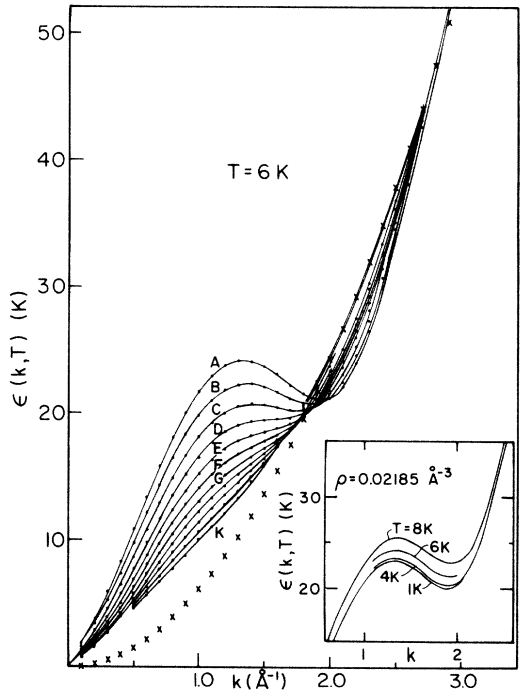

FIG. 3. Calculated excitation energies as a function of wave number k for ^{4}He at $T=6$ K for several densities (in Å^{-3}); *A*, 0.02185; *B*, 0.020; *C*, 0.018; *D*, 0.016; continuing to smaller densities in increments of 0.002 until density *K* of 0.002 Å^{-3}. The *x*'s lie on the free particle spectrum. The inset shows the same quantity at the experimental equilibrium density for several temperatures.

tion energies on temperature at fixed density $\rho=0.021\,85$ Å^{-3} is shown in the inset of Fig. 3. In contrast to the available experimental results[34] the theoretical roton energies increase with increasing temperature. This disagreement is expected since the observed lowering of the roton gap is attributed to roton-roton interactions which are not incorporated in the present model.

This property of the optimal excitation energies suppresses therefore any strong variation of the theoretical static structure function with temperature in the roton region. In qualitative accord with experimental results below the lambda temperature[34,35] we observe a monotonic increase of the peak value of our theoretical structure function with increasing temperature. However, we do not find a sharpening of this peak [see, in particular, Fig. 4(b)]. The numerical results do not indicate a reversal of this behavior in contrast to the experimental findings above the lambda transition. The structure function shows increasingly less structure with decreasing density. As can be seen in Fig. 5, at $T=5$ K and $\rho=0.002$ Å^{-3} the maximum which is present at liquid densities has almost disappeared and $S(k)$ comes very close to unity at all wave numbers except at k values in the phonon region $k<0.5$ Å^{-1} where the structure function approaches $S(k)=k_B T/mc^2$ as $k\to 0$. The strong temperature dependence of $S(k)$ at small k values at fixed density well away from the critical density (Fig. 4) is due largely to the factor of T which appears in the numerator of the zero k limit. On the other hand, if one fixes the temperature near the critical temperature as in Fig. 5 and varies the density, the $k=0$ intercept has a maximum at a density near the critical density. Indeed this density diverges at the calculated critical point, thus manifesting critical opalescence.

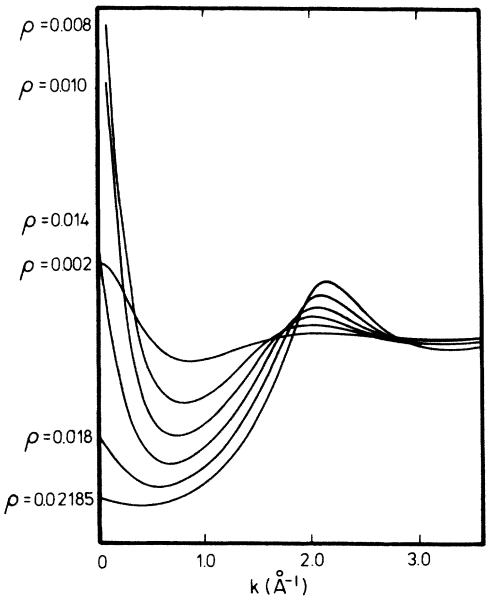

FIG. 5. Calculated ^{4}He structure function as a function of k at several different densities but for a fixed temperature of 5 K.

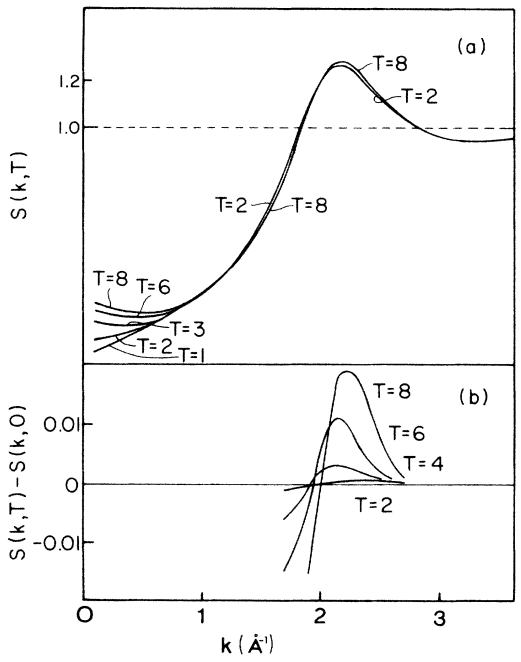

FIG. 4. (a) Calculated ^{4}He structure functions as functions of wave number k at experimental equilibrium density for several temperatures. (b) The difference between $S(k,T)$ and its $T=0$ value as a function of k at several different temperatures, plotted with an expanded vertical scale to illustrate this temperature dependence.

At constant density the calculated optimal radial distribution function $g(r)$ exhibits a more pronounced structure, i.e., higher maxima and lower minima, if the temperature is increased. The increase in structure is accompanied by a slight shift of the extrema to smaller relative distances. Both features are in qualitative agreement with experimental results (at temperatures below the lambda point).

V. OPTIMAL THERMODYNAMIC QUANTITIES

Having the optimal structure function, radial distribution function and the corresponding excitation energies for helium matter at our disposal we may calculate the associated optimal entropy (25), Helmholtz free energy (26), chemical potential (47), and the corresponding thermodynamic equation of state, $P=P(\rho,T)$. Some of our numerical results on these thermodynamic quantities for ^{4}He are depicted in Figs. 6, 7, and 8.

In the region of mechanical stability (where the velocity of sound c is well defined) the isotherms (isochors) of the calculated entropy density decrease (increase) monotonically with increasing density (temperature). The most remarkable feature of the entropy density is that it approaches a finite nonzero value as the particle density ρ vanishes. Thus, in this calculation, the vacuum possesses physical properties such as a nonvanishing entropy density, a finite energy density (Fig. 7), and a positive pressure (Fig. 8). These features are reminiscent of the ideal Bose

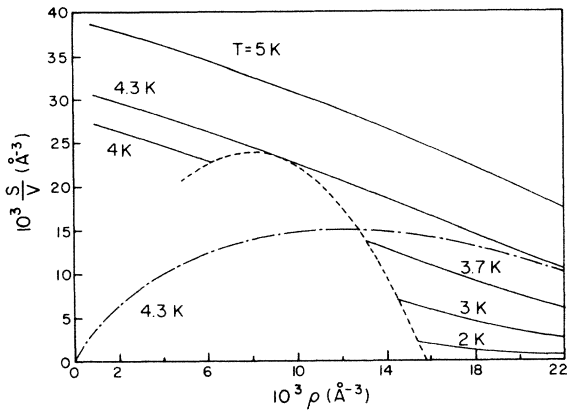

FIG. 6. Calculated ^{4}He entropy density isotherms as functions of density. The dashed line is the spinodal line. The dashed-dotted curve is the 4.3 K isotherm for the extended model of Sec. VI.

gas, except that in that case as one lowers the density at fixed temperature the phase boundary into the normal gas phase is crossed before one reaches the vacuum. Indeed, upon analyzing the temperature dependence of the results on the entropy density, free energy density, and pressure in the limit of vanishing particle density we find that these thermodynamic quantities represent very well the properties of a gas of noninteracting bosons with an effective mass m^* arrested in the superfluid phase. Thus the Helmholtz free energy density at $\rho=0$ is described by

$$\left.\frac{F}{V}\right|_{\rho=0} \equiv \frac{F_B}{V} = -\left[\frac{m^*}{2\pi\hbar^2}\right]^{3/2} \zeta_{5/2}(1)\beta^{-5/2} . \tag{48}$$

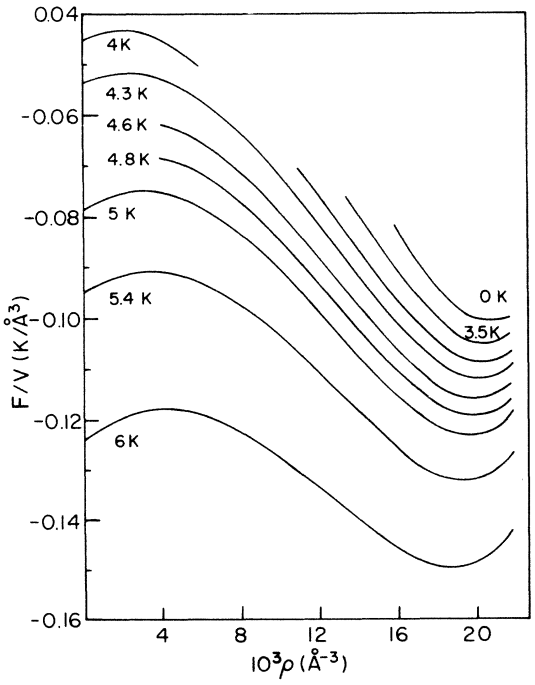

FIG. 7. Helmholtz free energy density as in Fig. 6.

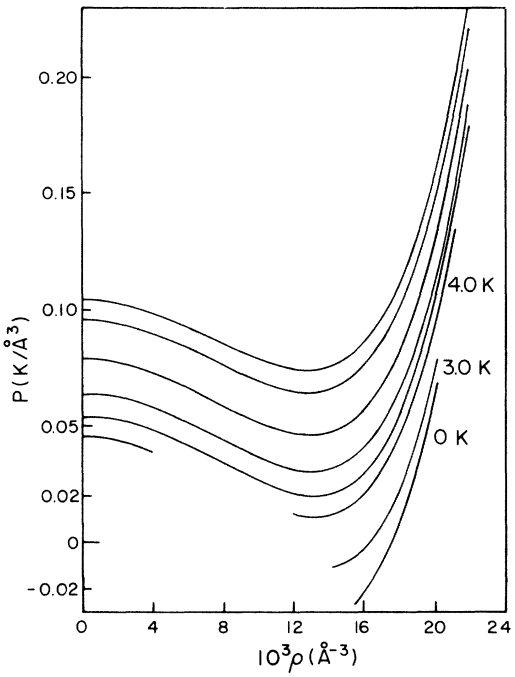

FIG. 8. Pressure as in Fig. 5.

Here, the function $\zeta_\sigma(z)=\sum_{n=1}^{\infty} z^n/n^\sigma$ and Eq. (48) represents the standard formula for noninteracting bosons of mass m^* at temperatures below the corresponding Bose transition temperature[36]

$$T^* = \frac{2\pi\hbar^2}{m^*}\left[\frac{\rho}{\zeta_{3/2}(1)}\right]^{2/3} . \tag{49}$$

The numerical results on the entropy density, internal energy density, and pressure as $\rho \to 0$ are then well reproduced by taking the appropriate derivatives of Eq. (48) with respect to temperature or density, respectively. A similar low-density behavior is found by analyzing our numerical results on the optimal entropy, free energy, and pressure for ^{6}He matter and extended systems of helium atoms with hypothetical mass m of two-thirds and one-half the ^{4}He mass. The numerical results on the corresponding effective masses m^* are collected in Table I. They fit the optimal data at $\rho=0$ very well at all temperatures considered. Thus, we may conclude that a system of bosons described by the Helmholtz free energy (26), with $\dot{D}_1$ set to zero and the optimal expressions (25) and (27) can coexist with a particular vacuum having physical properties described by Eq. (48). A double tangent method then permits the construction of a two-phase coexistence region in a standard fashion. The resulting phase boundary for ^{4}He is indicated by the nearly vertical dashed line in Fig. 1. The equilibrium state to the left of this line is, in this model, the liquid at the density of the dashed line in equilibrium with the vacuum which is characterized by Eq. (48). Consequently, if this construction yields a gas-liquid critical point at all it must be at very high temperature. This behavior is in clear disagreement with the results expected based upon the observed

TABLE I. Numerical results on the corresponding effective masses m^*.

m/m_4	$\frac{3}{2}$	1	$\frac{2}{3}$	$\frac{1}{2}$
m^*/m	0.586	0.787	0.795	0.812

physical situation or upon our earlier construction of a spinodal line and the associated critical point based on the stability criterion (42) and (43). However, this discrepancy is not unexpected and is caused by the limitations of ansatz (5) or (7) in conjunction with (2) and (9) for the trial density matrix. It is known that such an ansatz leads necessarily to a nonvanishing condensate fraction and is therefore unable to permit an adequate description of any normal (i.e., nonsuperfluid) phase which the helium systems considered here will certainly attain at sufficiently low densities. Moreover, the application of the present approximate model in the low density region at rather elevated temperatures is bound to violate the separability assumption. This approximation is valid essentially if the total number of elementary excitations, i.e., $\sum_{\mathbf{k}} n(k)$, is sufficiently small compared with the total number N of bosons contained in the system studied. It is obvious that this condition cannot be fulfilled at finite temperatures if the density ρ and therefore the total number of particles $N=\rho V$ vanishes while the number of excitations in our model approaches a positive value in this region of phase space. It is due to this inconsistency that our numerical results on the model free energy densities do not approach zero as $\rho\rightarrow 0$ but remain negative. The result tells us that the approximate energy density lies below the true one thus demonstrating that the upper bound property of Eq. (4) has been lost by assuming separability in this particular region of the ρ,T phase space.

To overcome these shortcomings of the present model we have (i) to explore more complex choices for functions Φ and Q in Eq. (5) which permit an adequate treatment of normal liquid or gaseous phases, and (ii) to improve upon the separability assumption (18) allowing for a systematic approximation scheme for evaluating the function $\dot{D}_1$ in Eq. (26).

Before turning to this more advanced stage of development we can do two things at present to help out and to guide future improvements. To learn something about the normal gas phase boundary we may employ the quantum virial expansion from which we can deduce the pressure and chemical potential of the low density phase at low temperatures. Alternatively, we may use the observations above about similarities of the results to an ideal Bose gas arrested in the Bose condensed state to make a heuristic modification of the present model which incorporates a transition to the normal phase and, consequently, a more realistic description of the two-phase region. This latter approach is developed in the next section.

The low temperature part of the phase boundary between the superfluid liquid and the normal gas may be estimated by using the quantum virial expansion for the gas phase equation of state. The procedure we adopt is to use this expansion in the form

$$P/k_BT=\lambda^{-3}\sum_{l=1}^{\infty} b_l z^l , \tag{50}$$

$$\rho=\lambda^{-3}\sum_{l=1}^{\infty} l b_l z^l , \tag{51}$$

where $\lambda=(2\pi\hbar^2/mk_BT)^{1/2}$ and the fugacity $z=\exp(\beta\mu)$. The first quantum virial coefficient $b_1=1$, while we obtain the second quantum virial coefficient b_2 for ^{4}He with the Lennard-Jones potential and the de Boer-Michels parameters from Ref. 37. Making use of the higher density data from above for P and ρ at specific values of T as a function of ρ, the above expressions truncated at the second virial term are used to find the liquid and gas values of ρ which define the phase boundary.

The results are shown as the solid lines in the lower half of Fig. 9. Of course the inaccuracy of the calculated ground-state binding energy of more than 2 K already makes the vapor pressure calculation error substantial because this same error appears in μ. Ground-state improvements are readily available[11] but are beyond the scope of the present calculation. Our long-range objective includes a variational ansatz which has the proper low density normal gas limit.

VI. NORMAL PHASE AT ELEVATED TEMPERATURES

In this section we make use of the low density results obtained in the variational calculation to make a heuristic extension of the model to include the normal phase in the part of the phase diagram which cannot be represented using the second-order virial expansion. In order to do this we are abandoning any reference to the variational principle or any direct relationship to a microscopic description of the system. Instead, we make use of the numerical data obtained above to decompose our results on thermo-

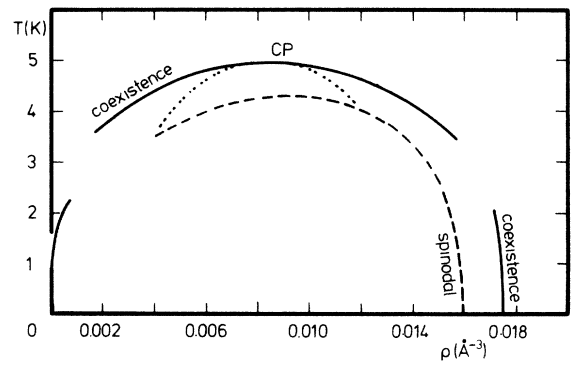

FIG. 9. The calculated liquid-gas phase diagram for ^{4}He. The dashed line is the ^{4}He isothermal spinodal line calculated with the model density matrix (8) the approximations of Sec. II. The solid line is the liquid-gas coexistence line calculated below $T=2.5$ K using the quantum virial expansion at low densities and the equation of state for our model density matrix at high densities; for $T>3$ K the liquid-gas coexistence line (solid line) is obtained using the heuristic extension described in Sec. VI. The dotted line is the corresponding isothermal spinodal line.

dynamic quantities such as S/V, F/V, or P into a kinetic piece resembling the (vacuum) contributions of a Bose gas of free particles with an effective mass m^* and a potential part which vanishes in the low density limit but survives at zero temperature. For example, we write the Helmholtz free energy in the form

$$\frac{F}{V}=\frac{F_B}{V}+\frac{F_W}{V}\ , \tag{52}$$

where the first term is defined by Eq. (48) or the equation of state,

$$P=P_B+P_W \tag{53}$$

with the partial pressure

$$P_B=\left[\frac{m^*}{2\pi\hbar^2}\right]^{3/2}\zeta_{5/2}(1)\beta^{-5/2}\ . \tag{54}$$

Extracting the piece P_W from our numerical results on the optimal pressure we find that this portion is almost independent of temperature (at least up to $T=6$ K) but is strongly dependent on density. Components F_B/V and S_B/V exhibit a similar behavior at temperatures which are not too low and where phonon effects are no longer important ($T\gtrsim 3$–4 K in this model). Decompositions (52) and (53) suggest a plausible phenomenological generalization to extend the present model to deal with the normal phase at low densities in a heuristic fashion. Following qualitatively the treatment and discussion of Ref. 38 we expect that the superfluid component with entropy S_B/V, energy density F_B/V, and pressure P_B undergoes, in reality, a transition to the normal phase at temperatures above the effective ideal Bose gas line, $T=T^*$, where the critical temperature should be roughly of the order given by expression (49). Adopting this plausible patchwork to extend the present microscopic model we then have to replace F_B, S_B, and P_B by the familiar results describing the normal behavior of independent bosons with an effective mass m^* if the temperature $T>T^*$, T^* defined by Eq. (49). This extension guarantees that the thermodynamic quantities considered, i.e., entropy density, free energy density, and pressure, behave normally and vanish as $\rho\to 0$. As an example, we have plotted in Fig. 6 the entropy at $T=4.3$ K as a function of density if the extended procedure described above is applied. The P,ρ phase diagram of this extended model for ^{4}He matter is presented in Fig. 10. In contrast to the optimal results on the equation of state (Fig. 8) which are based on the microscopic model (5)–(9) and Eq. (2) discussed above, the phenomenologically extended model generates isotherms which show the familiar form known from classical van der Waals theory.[39,40] Applying the standard Maxwell construction to these results yields a coexistence curve which is represented in Fig. 10 by the dashed curve. Its maximum gives the gas-liquid critical data for the extended model. Table II collects these results for ^{4}He and the experimental data in reduced units.[33] Comparing these data we find that the crude phenomenological extension of the model reproduces the experimental data fairly well.

The location of the coexistence line for the extended model in the T,ρ phase diagram is depicted in the upper half of Fig. 9. The corresponding instability curve in which the isothermal compressibility becomes infinite in this model is indicated by a dotted line. This curve should be compared with the spinodal line (dashed curve) which is based on the stability condition (43) representing the points in the T,ρ space where the velocity c of the elementary excitations vanishes. If the models considered were exact both spinodal curves would coincide. However, they differ in general if an approximate density matrix is employed. This feature is well known from variational studies of the ground state of liquid ^{4}He.[32]

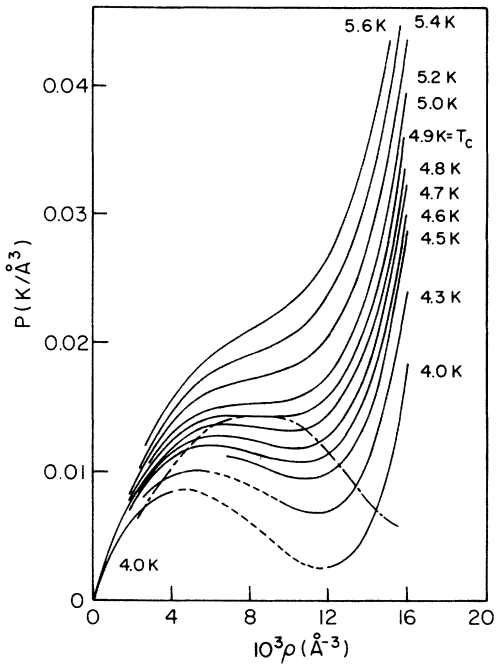

FIG. 10. Pressure isotherms for the extended model of Sec. VI. The dashed-dotted curve is the corresponding liquid-gas coexistence curve.

VII. DISCUSSION

We have presented here a first-principles derivation of the liquid-gas portion of the phase diagram of liquid ^{4}He, as well as similar information for two other boson isotopes of helium. The most important part of this work is the demonstration that one can begin from a plausible model of the coordinate space representation of the density matrix and, using the variational principle for the Helmholtz free energy, arrive at a semiquantitative account of some of the properties of the fluid. To our

TABLE II. Results for ^{4}He and the experimental data in reduced units.

	T_c^*	ρ_c^*	P_c^*	$\rho_c T_c/P_c$
^{4}He	0.48	0.15	0.024	3.0
^{4}He (experiment)	0.51	0.17	0.027	3.21

knowledge, this is the only first-principles theoretical determination of the critical point of ^{4}He.

The theoretical treatment presented here is only a beginning. Approximations are used which should be improved. The model density matrix is also less than adequate for a quantitative treatment of the liquid-gas properties, and for even a qualitative treatment of the lambda transition.

It may be worthwhile mentioning some of the improvements which can be applied.

The two-body potential energy used in these calculations was the Lennard-Jones 6-12 potential. While this has some formal advantages, it is now generally believed that the (Hartree-Fock-dispersion) HFDHE2 two-body potential of Aziz *et al.*[41] is superior. Future calculations which improve on the above results should incorporate that potential, although the present level of approximation does not merit that care.

The hypernetted-chain (HNC) approximation is a calculational convenience which, however, leads to a ground-state binding energy error of approximately 1 K. Since this error also appears in the chemical potential, it seriously affects the vapor-pressure calculation in the virial expansion. This situation can be improved by including elementary diagrams in the HNC equation,[42] or by replacing the HNC approach by a Monte Carlo simulation.[43]

It was necessary to introduce the separability approximation in order to calculate the entropy as a function of $u(r)$ and $\gamma(r)$. Besides making the entropy calculation feasible, this approximation produces a physically plausible and intuitively appealing set of equations which makes the interpretation of the results straightforward. However, this approximation is the most difficult to justify (except at long wavelengths) and improve. This should be a fertile ground for further improvements.

The advantage of the particular structure chosen for the variational density matrix in the present work is not only its simplicity. It also contains the correct low-temperature limit of the incoherence factor Q. This structure of Q, along with the temperature dependence of $u(r)$ and $\gamma(r)$, was derived originally by Reatto and Chester[19] from considerations of the cluster expansion of the exact density matrix. They also showed how the long-range structure of $u(r)$ and $\gamma(r)$ is determined by the phonon dispersion relation. It is reassuring that our variational calculations clearly reproduce this analytic structure, i.e., the solutions to the variational equations have the proper long-range structure. It is also reassuring to note that the approximations used—HNC and separability—do not damage this result; this feature was already known, however, in the ground-state calculations.[8,12]

The particular structure of our trial density matrix is a major limitation in itself. Some quantitative improvement may be obtained by adopting procedures already well established in the ground-state problem. In particular, the inclusion of three-body factors in Φ will give the same improvement at low temperatures as it did in the ground-state calculation.[11] However, the temperature dependence should be more dramatically affected by introducing the same physical processes into the elementary excitation spectrum,[11] which in this density matrix approach is accomplished by including appropriate factors in $Q(\underline{R},\underline{R}')$. In the sense that $\gamma(r)$ is really a correlation between a primed and an unprimed "particle," it thus more generally should be written as

$$\gamma(\mathbf{r}-\mathbf{r}')=\gamma_{1;1}(\mathbf{r},\mathbf{r}') \ . \tag{55}$$

The three-body factors in Φ should have their analogues in Q in the form of $\gamma_{1;2}(\mathbf{r}_1;\mathbf{r}_1',\mathbf{r}_2')$ terms in the exponential; in Ref. 5 it is shown how this arises naturally out of the backflow terms in the elementary excitations. Similarly, elementary excitation interactions would require $\gamma_{2;2}$ terms. In summary, the general structure of Q has the form

$$Q(\underline{R},\underline{R}')=\exp\left[\sum_{m,n=1}^{N}\sum_{\underline{R}^{(m)},\underline{R}'^{(n)}}\gamma_{m;n}(\underline{R}^{(m)};\underline{R}'^{(n)})\right] , \tag{56}$$

where $\underline{R}^{(n)}$ refers to the coordinate subset $\mathbf{r}_{i_1},\ldots,\mathbf{r}_{i_n}$, and the second summation sign represents the sum over all distinct choices of these subsets from the primed and from the unprimed sets. A similar expression for Φ is just the familiar Feenberg function studied in the ground-state problem. On present computers this approach should be practical through terms satisfying $n+m=4$.

An alternative method which contains the same general information would be to generalize Pandharipande's momentum-dependent Jastrow function to the density matrix.[44] Including the momentum operator in Φ would have the effect of generating higher index factors in Q, similar to the ones discussed above and in Ref. 5.

While these improvements of the density matrix will lead to quantitative improvement in the liquid-gas region, they will almost certainly not correct the chief deficiency of the present theory, namely, the absence of evidence for the off-diagonal long-range-order transition corresponding to the lambda transition. Specifically, we conjecture that, in three dimensions, a finite truncation of $n+m$ will always produce a density matrix which has a finite Bose-Einstein condensate fraction. The proof is the same as for the corresponding theorem for Jastrow functions.[45] It depends in an essential way on the large r behavior of $u(r)$ and $\gamma(r)$, and in fact could be reinterpreted as a proof that the disappearance of the condensate would correspond to the onset of an asymptotic divergence in these functions. A particular example of this was given by Reatto and Chester in Ref. 19, where they showed that the thermally populated phonons deplete the condensate at any nonzero temperature in two dimensions, and that this is accomplished analytically by the density matrix of the form of Eqs. (2), (5), and (6) by virtue of the fact that $u(r)$ and $\gamma(r)$ diverge as $\ln r$ at large r. Our variational method produces the same results in two dimensions.[46]

While one cannot *a priori* rule out a similar occurrence at some finite temperature in three dimensions for some $\gamma_{n;m}$ and/or u_n, there is no evidence in the analytic structure of the equations we have derived that this will take place, nor is it plausible that this would be the analytic manifestation of the physical situation.

Additional insight into the general structure may be obtained by taking the high-temperature limit of the exact

density matrix. Following the arguments of Kirkwood,[47] one can easily show that

$$\lim_{T\to\infty}\Phi(\underline{R})=e^{-\beta V(\underline{R})/2}, \tag{57}$$

where $V(\underline{R})$ is the potential energy of configuration $\underline{R}$, and thus has the Jastrow structure with $u(r,T)=-\beta v(r)/2$. On the other hand, the incoherence factor does not have the structure which we have used in the present work, but has instead the structure of a permanent:

$$\lim_{T\to\infty}Q(\underline{R},\underline{R}')=\mathrm{Perm}\Gamma(\mathbf{r}_i-\mathbf{r}'_j), \tag{58}$$

where, in this limit,

$$\Gamma(r)=e^{-\pi r^2/\lambda^2}, \tag{59}$$

where lambda is the thermal de Broglie wavelength. It is the fact that $\Gamma(r)$ is a finite ranged function which destroys the condensate fraction.

Clearly the two-body product form we have used in this work cannot evolve into this permanent form. Moreover, although this permanent is positive when the above form for Γ is employed, there appears to be no finite truncation of the exponentiated series which produces a good approximation to this form.

These observations suggest that an appropriate generalization of the trial density matrix which may represent the lambda transition would be to include the permanent factor in Q, with $\Gamma(r)$ being a variational function. At low temperatures one would expect $\Gamma(R)$ to approach a nonzero limit at large r, while the high-temperature limit should be Eq. (59). The lambda transition would then correspond to the transition between these behaviors. Indeed one can see from this discussion that $\Gamma(r)$ should behave very much like the reduced one-body density matrix. Carrying out a program to evaluate the free energy as a functional of $\Gamma(r)$ is well beyond the scope of the work reported here, since it entails developing an appropriate mathematical scheme to include the effects of the permanent.

ACKNOWLEDGMENTS

One of us (C.E.C.) would like to acknowledge the support of the Alexander von Humboldt-Stiftung (Bonn, Germany) and the hospitality of the Institute for Theoretical Physics of the University of Cologne during the initial phase of this research. Part of this work was done while M.L.R. was enjoying the hospitality of the School of Physics, the University of New South Wales, Australia, where he was visiting. We thank G. V. Chester, H. Falk, A. Huber, D. Neilson, L. Nosanow, J. Percus, L. Reatto, and V. Sears for informative discussions. In addition to the above-mentioned support, this work has been supported in part by the National Science Foundation under Grants No. DMR-77-18329 and No. DMR-79-26447, by the U.S. Department of Energy through Contract No. DE-AC02-76ER03077 and by the Deutsche Forschungsgemeinschaft (Bonn, W. Germany) under Grant No. Ri-267.

*Present address: Institut für Theoretische Physik, Universität zu Köln, D-5000 Köln 41, West Germany.

[1]*Lecture Notes in Physics, Recent Progress in Many-Body Theories,* edited by H. Kümmel and M. L. Ristig (Springer, Berlin, 1984), Vol. 198.

[2]P. A. Whitlock, M. H. Kalos, and G. V. Chester, J. Stat. Phys. **32**, 389 (1983).

[3]E. L. Pollock and D. M. Ceperley, Phys. Rev. B **30**, 2555 (1984).

[4]G. Gaglione, G. L. Masserini, and L. Reatto, Phys. Rev. B **23**, 1129 (1981).

[5]S. Battaini and L. Reatto, Phys. Rev. B **28**, 1263 (1983).

[6]M. Puoskari, A. Kallio, and P. Pollari (unpublished).

[7]E. Feenberg, *Theory of Quantum Fluids* (Academic, New York, 1969).

[8]C. E. Campbell, in *Progress in Liquid Physics,* edited by C. A. Croxton (Wiley, New York, 1978); C. E. Campbell and F. J. Pinski, Nucl. Phys. **A328**, 210 (1979).

[9]C. W. Woo, Phys. Rev. Lett. **28**, 1442 (1972).

[10]C. E. Campbell, Phys. Lett. **44A**, 471 (1973).

[11]C. C. Chang and C. E. Campbell, Phys. Rev. B **15**, 4238 (1977).

[12]C. E. Campbell and E. Feenberg, Phys. Rev. **188**, 396 (1969).

[13]A. Huber, in *Methods and Problems of Theoretical Physics,* edited by J. E. Bowcock (North-Holland, Amsterdam, 1970), Vol. 37.

[14]C. E. Campbell, K. E. Kürten, M. L. Ristig, and G. Senger, Phys. Rev. B **30**, 3728 (1984).

[15]C. E. Campbell, M. L. Ristig, K. E. Kürten, and G. Senger, in *Proceedings of the 17th International Conference on Low Temperature Physics,* edited by U. Eckern, A. Schmid, W. Weber, and H. Wühl (Elsevier, New York, 1984).

[16]M. L. Ristig, G. Senger, K. E. Kürten, and C. E. Campbell, in *Proceedings of the 17th International Conference on Low Temperature Physics,* edited by U. Eckern, A. Schmid, W. Weber, and H. Wühl (Elsevier, New York, 1984).

[17]G. Senger, Diplomarbeit 1984, Universität zu Köln (unpublished).

[18]C. E. Campbell, J. Math. Phys. **16**, 1076 (1975).

[19]L. Reatto and G. V. Chester, Phys. Rev. **155**, 88 (1967).

[20]E. Feenberg, Ann. Phys. (N.Y.) **70**, 133 (1972).

[21]C. DeMichelis, G. Masserini, and L. Reatto, Phys. Rev. A **18**, 296 (1978).

[22]C. DeMichelis, G. Masserini, and L. Reatto, Phys. Lett. **66A**, 484 (1978).

[23]T. Morita and K. Hiroike, Prog. Theor. Phys. **23**, 1003 (1960).

[24]K. Hiroike, Prog. Theor. Phys. **24**, 317 (1960).

[25]C. E. Campbell, Ann. Phys. (N.Y.) **74**, 43 (1972).

[26]P. C. Martin, in *Many-Body Physics,* edited by C. DeWitt and R. Balian (Gordon and Breach, New York, 1968), Vol. 37.

[27]K. E. Kürten and C. E. Campbell, Phys. Rev. B **26**, 124 (1982).

[28]P. R. Zilsel, in *The Many-Body Problem,* edited by J. K. Percus (Wiley, New York, 1963).

[29]N. N. Bogoliubov, *Lectures on Quantum Statistics* (Gordon and Breach, New York, 1967), Vol. 1.
[30]E. Krotscheck, G.-X. Qian, and W. Kohn, Phys. Rev. B **31**, 4245 (1985).
[31]P. Y. Siemens and L. J. Lantto, Phys. Lett. **68B**, 308 (1977).
[32]A. D. Jackson, A. Lande, and L. J. Lantto, Nucl. Phys. **A317**, 70 (1979).
[33]L. H. Nosanow, J. Low Temp. Phys. **23**, 605 (1976); M. D. Miller, L. H. Nosanow, and L. J. Parish, Phys. Rev. Lett. **35**, 581 (1975).
[34]E. C. Svensson and A. F. Murray, Physica **108B**, 1317 (1981).
[35]F. W. Wirth, D. A. Ewen, and R. B. Hallock, Phys. Rev. B **27**, 5530 (1983).
[36]F. London, *Superfluids* (Wiley, New York, 1954), Vol. 2.
[37]J. E. Kilpatrick, W. E. Keller, E. F. Hammel, and N. Metropolis, Phys. Rev. **94**, 1103 (1954).
[38]K. Huang, Phys. Rev. **119**, 1129 (1960); and in *Studies in Statistical Mechanics,* edited by J. de Boer and G. E. Uhlenbeck (North-Holland, Amsterdam, 1964).
[39]P. A. Egelstaff, *An Introduction to the Liquid State* (Academic, London, 1967).
[40]T. Hill, J. Phys. Chem. **51**, 1219 (1947).
[41]R. A. Aziz, V. P. S. Nain, J. S. Carley, W. J. Taylor, and G. T. McConville, J. Chem. Phys. **70**, 4330 (1979).
[42]R. A. Smith, A. Kallio, M. Puoskari, and P. Toropainen, Nucl. Phys. **A328**, 186 (1979).
[43]F. J. Pinski and C. E. Campbell, Phys. Lett. **79B**, 23 (1978).
[44]V. R. Pandharipande, Phys. Rev. B **18**, 218 (1978).
[45]L. Reatto, Phys. Rev. **183**, 334 (1969).
[46]P. M. Lam, Z. Phys. **48**, 51 (1982).
[47]J. G. Kirkwood, Phys. Rev. **44**, 31 (1933).